Ruthenium(II) σ-Acetylide and Carbene Complexes Supported by the Terpyridine−Bipyridine Ligand Set: Structural, Spectroscopic, and Photochemical Studies†

Chun-Yuen Wong, Michael C. W. Chan, Nianyong Zhu, and Chi-Ming Che*

Department of Chemistry and HKU-CAS Joint Laboratory on New Materials, The University of Hong Kong, Pokfulam Road, Hong Kong SAR, China

Received December 17, 2003

A series of acetylide- and carbene-ruthenium complexes containing polypyridine ligands, $[(tpy)(bpy)RuC{\equiv}CR]^+$ (tpy = 2,2′:6′,2″-terpyridine, bpy = 2,2′-bipyridine; R = C_6H_4F-4 (**1**), C_6H_4Cl-4 (**2**), C_6H_5 (**3**), C_6H_4Me-4 (**4**), C_6H_4OMe-4 (**5**), *t*-Bu (**6**), $(C_6H_4C{\equiv}C)_nC_6H_5$ [*n* = 1 (**7**) and 2 (**8**)]) and $[(tpy)(bpy)Ru{=}C(OMe)(CH_2R)]^{2+}$ (R = C_6H_4OMe-4 (**9**), *t*-Bu (**10**)) have been prepared. The molecular structures of **4**(PF_6), **5**(PF_6), and **9**$(ClO_4)_2$ reveal Ru−C distances of 2.025(9), 2.025(7), and 1.933(6) Å, respectively. The Ru(III/II) oxidation waves are irreversible for **1**−**8** (E_{pa} = 0.15−0.26 V vs $FeCp_2^{+/0}$) but reversible for **9** and **10** ($E_{1/2}$ = 0.99 and 1.00 V, respectively). The absorption bands in the visible region for **1**−**8** (λ_{max} = 502−526 nm) and **9** and **10** (λ_{max} ca. 410 nm) are assigned as $d_\pi(Ru^{II}) \rightarrow \pi^*$(polypyridine) MLCT transitions. Complexes **1**−**8** weakly emit at λ_{max} = 748−786 nm in CH_3CN solution at 298 K (λ_{ex} = 550 nm). Complexes **9** and **10** are nonemissive in CH_2Cl_2 solution at 298 K, but in glassy *n*-butyronitrile at 77 K, excitation at λ = 415 nm produces emission at λ_{max} = 597 and 615 nm, respectively. These emissions are tentatively ascribed as $d_\pi(Ru^{II}) \rightarrow \pi^*$(polypyridyl) ^{3}MLCT in nature. The carbene derivatives **9** and **10** undergo photochemical reactions upon irradiation in solution, and $[(tpy)(bpy)RuN{\equiv}CCH_3]^{2+}$ and 4-methoxybenzaldehyde were isolated from the photolysis of **9** in CH_3CN.

Introduction

Ruthenium complexes containing aromatic diimine or polypyridyl ligands have been a focal point for investigations in many research topics including photochemistry,[1] electron transfer reactions,[2] luminescent sensing,[3] light-emitting devices,[4] and photosensitizers.[5] The attention devoted to ruthenium(II) complexes supported by aromatic diimine ligands has arisen because they exhibit rich photophysical and photochemical properties, which originate from the triplet $[d_\pi(Ru^{II}) \rightarrow \pi^*$(aromatic diimine)] metal-to-ligand charge transfer (MLCT) excited state, the prototypical example being $[Ru(bpy)_3]^{2+}$ (bpy = 2,2′-bipyridine). Hence, the long-lived emissive ^{3}MLCT excited state of $[Ru(bpy)_3]^{2+}$ and its derivatives have found important applications in many disciplines.[6] Ruthenium(II) complexes bearing tridentate polypyridine ligands such as $[Ru(tpy)_2]^{2+}$ (tpy = 2,2′:6′,2″-

† The "Ru=C" formalism is used for the ruthenium-carbene moiety to denote a single σ-bond with π-back-bonding character.

(1) (a) Kalyanasundaram, K. *Coord. Chem. Rev.* **1982**, *46*, 159. (b) Juris, A.; Balzani, V.; Barigelletti, F.; Campagna, S.; Belser, P.; von Zelewsky, A. *Coord. Chem. Rev.* **1988**, *84*, 85. (c) Balzani, V.; Barigelletti, F.; De Cola, L. *Top. Curr. Chem.* **1990**, *158*, 31. (d) Sauvage, J.-P.; Collin, J.-P.; Chambron, J.-C.; Guillerez, S.; Coudret, C.; Balzani, V.; Barigelletti, F.; De Cola, L.; Flamigni, L. *Chem. Rev.* **1994**, *94*, 993.

(2) (a) Meyer, T. J. *Acc. Chem. Res.* **1989**, *22*, 163. (b) Balzani, V.; Juris, A.; Venturi, M.; Campagna, S.; Serroni, S. *Chem. Rev.* **1996**, *96*, 759. (c) De Cola, L.; Belser, P. *Coord. Chem. Rev.* **1998**, *177*, 301.

(3) (a) Balzani, V.; Sabbatini, N.; Scandola, F. *Chem. Rev.* **1986**, *86*, 319. (b) de Silva, A. P.; Gunaratne, H. Q. N.; Gunnlaugsson, T.; Huxley, A. J. M.; McCoy, C. P.; Rademacher, J. T.; Rice, T. E. *Chem. Rev.* **1997**, *97*, 1515.

(4) (a) Lee, J.-K.; Yoo, D. S.; Handy, E. S.; Rubner, M. F. *Appl. Phys. Lett.* **1996**, *69*, 1686. (b) Elliott, C. M.; Pichot, F.; Bloom, C. J.; Rider, L. S. *J. Am. Chem. Soc.* **1998**, *120*, 6781. (c) Handy, E. S.; Pal, A. J.; Rubner, M. F. *J. Am. Chem. Soc.* **1999**, *121*, 3525. (d) Buda, M.; Kalyuzhny, G.; Bard, A. J. *J. Am. Chem. Soc.* **2002**, *124*, 6090. (e) Bernhard, S.; Barron, J. A.; Houston, P. L.; Abruña, H. D.; Ruglovksy, J. L.; Gao, X.; Malliaras, G. G. *J. Am. Chem. Soc.* **2002**, *124*, 13624.

(5) (a) O'Regan, B.; Grätzel, M. *Nature* **1991**, *353*, 737. (b) Nazeeruddin, M. K.; Kay, A.; Rodicio, I.; Humphry-Baker, R.; Müller, E.; Liska, P.; Vlachopoulos, N.; Grätzel, M. *J. Am. Chem. Soc.* **1993**, *115*, 6382. (c) Bignozzi, C. A.; Schoonover, J. R.; Scandola, F. *Prog. Inorg. Chem.* **1997**, *44*, 1. (d) Gerfin, T.; Grätzel, M.; Walder, L. *Prog. Inorg. Chem.* **1997**, *44*, 345. (e) Kalyanasundaram, K.; Grätzel, M. *Coord. Chem. Rev.* **1998**, *177*, 347. (f) Bach, U.; Lupo, D.; Comte, P.; Moser, J. E.; Weissörtel, F.; Salbeck, J.; Spreitzer, H.; Grätzel, M. *Nature* **1998**, *395*, 583. (g) Hagfeldt, A.; Grätzel, M. *Acc. Chem. Res.* **2000**, *33*, 269.

(6) For recent works, see: (a) Sykora, M.; Kincaid, J. R. *Nature* **1997**, *387*, 162. (b) Sun, L.; Berglund, H.; Davydov, R.; Norrby, T.; Hammarström, L.; Korall, P.; Börje, A.; Philouze, C.; Berg, K.; Tran, A.; Andersson, M.; Stenhagen, G.; Mårtensson, J.; Almgren, M.; Styring, S.; Åkermark, B. *J. Am. Chem. Soc.* **1997**, *119*, 6996. (c) Beer, P. D.; Szemes, F.; Balzani, V.; Salà, C. M.; Drew, M. G. B.; Dent, S. W.; Maestri, M. *J. Am. Chem. Soc.* **1997**, *119*, 11864. (d) Lee, J.-K.; Yoo, D.; Rubner, M. F. *Chem. Mater.* **1997**, *9*, 1710. (e) Watanabe, S.; Onogawa, O.; Komatsu, Y.; Yoshida, K. *J. Am. Chem. Soc.* **1998**, *120*, 229. (f) Wu, A.; Yoo, D.; Lee, J.-K.; Rubner, M. F. *J. Am. Chem. Soc.* **1999**, *121*, 4883. (g) Farzad, F.; Thompson, D. W.; Kelly, C. A.; Meyer, G. J. *J. Am. Chem. Soc.* **1999**, *121*, 5577. (h) Liebsch, G.; Klimant, I.; Wolfbeis, O. S. *Adv. Mater.* **1999**, *11*, 1296. (i) Gao, F. G.; Bard, A. J. *J. Am. Chem. Soc.* **2000**, *122*, 7426. (j) Nazeeruddin, M. K.; Péchy, P.; Renouard, T.; Zakeeruddin, S. M.; Humphry-Baker, R.; Comte, P.; Liska, P.; Cevey, L.; Costa, E.; Shklover, V.; Spiccia, L.; Deacon, G. B.; Bignozzi, C. A.; Grätzel, M. *J. Am. Chem. Soc.* **2001**, *123*, 1613. (k) Watanabe, S.; Ikishima, S.; Matsuo, T.; Yoshida, K. *J. Am. Chem. Soc.* **2001**, *123*, 8402. (l) Rudmann, H.; Shimada, S.; Rubner, M. F. *J. Am. Chem. Soc.* **2002**, *124*, 4918. (m) Anzenbacher, P., Jr.; Tyson, D. S.; Jursíková, K.; Castellano, F. N. *J. Am. Chem. Soc.* **2002**, *124*, 6232. (n) Galoppini, E.; Guo, W.; Zhang, W.; Hoertz, P. G.; Qu, P.; Meyer, G. J. *J. Am. Chem. Soc.* **2002**, *124*, 7801. (o) Zhan, W.; Alvarez, J.; Crooks, R. M. *J. Am. Chem. Soc.* **2002**, *124*, 13265. (p) Potvin, P. G.; Luyen, P. U.; Bräckow, J. *J. Am. Chem. Soc.* **2003**, *125*, 4894. (q) Kalyuzhny, G.; Buda, M.; McNeill, J.; Barbara, P.; Bard, A. J. *J. Am. Chem. Soc.* **2003**, *125*, 6272. (r) Welter, S.; Brunner, K.; Hofstraat, J. W.; De Cola, L. *Nature* **2003**, *421*, 54.

10.1021/om034379k CCC: $27.50
Publication on Web 04/03/2004

terpyridine) have recently attracted interest as building blocks for the fabrication of linear molecular rods/wires for vectorial energy and electron transfer processes.[7] Meanwhile, the pursuit of $[Ru(bpy)_3]^{2+}$-related complexes exhibiting desirable and unprecedented photophysical characteristics continues unabated.[8]

Polypyridyl auxiliaries act as π-acidic and oxidatively robust ligands upon coordination to the ruthenium ion. In the literature, reports on highly oxidizing and isolable Ru=O complexes bearing polypyridyl ligands, such as $[(tpy)(bpy)Ru{=}O]^{2+}$,[9] have appeared. The oxidation chemistry of these Ru=O complexes has significantly impacted organic oxidation reactions over many years,[10] and their DNA cleavage capabilities have been recently highlighted.[11] We regard ruthenium−carbon multiply bonded species supported by the tpy-bpy ligand set as an interesting class of compounds. First, they may exhibit group transfer reactivities analogous to the oxygen atom transfer chemistry of the Ru=O congeners. Second, the electrochemistry and photophysics of $[(tpy)(bpy)RuL]^{n+}$ species (L = anionic or neutral donor) are well established, thus the nature of the ruthenium−carbon bonding interaction for organoruthenium derivatives can be probed spectroscopically and electrochemically by comparisons with known relatives. Third, it may be feasible to generate highly reactive ruthenium−carbon bonded species upon photoexcitation of the Ru → π^*(polypyridyl) charge transfer state. Incorporation of carbon-rich π-extended conjugated ligands into ruthenium-polypyridine moieties can yield new classes of emissive organoruthenium compounds with potential applications in material science. We therefore initiated a program directed toward the synthetic chemistry of organoruthenium complexes based on polypyridyl ancillary ligands. Significantly, reports on the preparation and characterization of tpy-bpy ruthenium derivatives bearing organometallic-type ligands are conspicuous by their rarity.[12] We now describe the synthesis of a series of acetylide- and carbene-ruthenium complexes containing the bpy and tpy auxiliaries. The structural, electrochemical, photophysical, and photochemical properties of these complexes, plus comparisons with $[Ru(tpy)(bpy)L]^{n+}$ analogues (L = anionic or neutral donor), are presented.

Experimental Section

General Procedures. All reactions were performed under a nitrogen atmosphere using standard Schlenk techniques unless otherwise stated. All reagents were used as received, and solvents were purified by standard methods. $[Ru(tpy)(bpy)(OH_2)](Y)_2$ (Y = ClO_4^-, PF_6^-) were prepared according to published procedures.[13] (**Caution!** *Perchlorate salts are potentially explosive and should be handled with care and in small amounts.*)

Physical Measurements and Instrumentation. ^1H, $^{13}C\{^1H\}$, $^1H-^1H$ COSY, $^1H-^1H$ NOESY, and $^{13}C-^1H$ COSY NMR spectra were recorded on Bruker 500 DRX and 600 DRX FT-NMR spectrometers. Peak positions were calibrated with Me_4Si as internal standard. Fast atom bombardment (FAB) mass spectra were obtained on a Finnigan MAT 95 mass spectrometer with 3-nitrobenzyl alcohol matrix. Infrared spectra were recorded as KBr plates on a Bio-Rad FT-IR spectrometer. UV−visible spectra were recorded on a Hewlett-Packard HP8452A diode array spectrophotometer interfaced with an IBM-compatible PC. Elemental analyses were performed by the Institute of Chemistry of the Chinese Academy of Sciences in Beijing.

Photoluminescence Measurements. Steady-state emission spectra were obtained on a SPEX Fluorolog-2 Model F111 fluorescence spectrophotometer. Low-temperature (77 K) emission spectra for glasses and solid-state samples were recorded in 5 mm diameter quartz tubes, which were placed in a liquid nitrogen Dewar equipped with quartz windows. Sample and standard solutions were degassed with at least three freeze−pump−thaw cycles. The emission quantum yield was measured by the method of Demas and Crosby[14] with $[Ru(bpy)_3](PF_6)_2$ in degassed CH_3CN as standard ($\Phi_r = 0.062$) and calculated by $\Phi_s = \Phi_r(B_r/B_s)(n_s/n_r)^2(D_s/D_r)$, where the subscripts s and r refer to sample and reference standard solution, respectively, n is the refractive index of the solvents, D is the integrated intensity, and Φ is the luminescence quantum yield. The quantity B is calculated by $B = 1 - 10^{-AL}$, where A is the absorbance at the excitation wavelength and L is the optical path length. Emission lifetime measurements were performed with a Quanta Ray DCR-3 pulsed Nd:YAG laser system (pulse output 355 nm, 8 ns). Errors for λ values (±1 nm), τ (±10%), and Φ (±10%) are estimated.

Electrochemical Measurements. Cyclic voltammetry was performed with a Princeton Applied Research Model 273A potentiostat. A conventional two-compartment electrochemical cell was used. The glassy-carbon electrode was polished with

(7) (a) Schwab, P. F. H.; Levin, M. D.; Michl, J. *Chem. Rev.* **1999**, *99*, 1863. (b) Harriman, A.; Khatyr, A.; Ziessel, R.; Benniston, A. C. *Angew. Chem., Int. Ed.* **2000**, *39*, 4287. (c) El-ghayoury, A.; Harriman, A.; Khatyr, A.; Ziessel, R. *Angew. Chem., Int. Ed.* **2000**, *39*, 185. (d) Passalacqua, R.; Loiseau, F.; Campagna, S.; Fang, Y.-Q.; Hanan, G. S. *Angew. Chem., Int. Ed.* **2003**, *42*, 1608.

(8) (a) Collin, J.-P.; Kayhanian, R.; Sauvage, J.-P.; Calogero, G.; Barigelletti, F.; Cian, A. D.; Fischer, J. *Chem. Commun.* **1997**, 775. (b) Barigelletti, F.; Flamigni, L.; Calogero, G.; Hammarström, L.; Sauvage, J.-P.; Collin, J.-P. *Chem. Commun.* **1998**, 2333. (c) Harriman, A.; Hissler, M.; Trompette, O.; Ziessel, R. *J. Am. Chem. Soc.* **1999**, *121*, 2516. (d) Harriman, A.; Hissler, M.; Khatyr, A.; Ziessel, R. *Chem. Commun.* **1999**, 735. (e) Fang, Y.-Q.; Taylor, N. J.; Hanan, G. S.; Loiseau, F.; Passalacqua, R.; Campagna, S.; Nierengarten, H.; Dorsselaer, A. V. *J. Am. Chem. Soc.* **2002**, *124*, 7912. (f) Polson, M. I.; Taylor, N. J.; Hanan, G. S. *Chem. Commun.* **2002**, 1356. (g) McClenaghan, N. D.; Passalacqua, R.; Loiseau, F.; Campagna, S.; Verheyde, B.; Hameurlaine, A.; Dehaen, W. *J. Am. Chem. Soc.* **2003**, *125*, 5356. (h) Schofield, E. R.; Collin, J.-P.; Gruber, N.; Sauvage, J.-P. *Chem. Commun.* **2003**, 188.

(9) (a) Moyer, B. A.; Thompson, M. S.; Meyer, T. J. *J. Am. Chem. Soc.* **1980**, *102*, 2310. (b) Thompson, M. S.; Meyer, T. J. *J. Am. Chem. Soc.* **1982**, *104*, 4106. (c) Thompson, M. S.; Meyer, T. J. *J. Am. Chem. Soc.* **1982**, *104*, 5070. (d) Thompson, M. S.; Giovani, W. F. D.; Moyer, B. A.; Meyer, T. J. *J. Org. Chem.* **1984**, *49*, 4972.

(10) (a) Che, C.-M.; Yam, V. W.-W. *Adv. Inorg. Chem.* **1992**, *39*, 233. (b) Griffith, W. P. *Chem. Soc. Rev.* **1992**, 179. (c) Goldstein, A. S.; Beer, R. H.; Drago, R. S. *J. Am. Chem. Soc.* **1994**, *116*, 2424. (d) Bailey, A. J.; Griffith, W. P.; Savage, P. D. *J. Chem. Soc., Dalton Trans.* **1995**, 3537. (e) Che, C.-M.; Cheng, K.-W.; Chan, M. C. W.; Lau, T.-C.; Mak, C.-K. *J. Org. Chem.* **2000**, *65*, 7996. (f) Che, C.-M.; Yu, W.-Y.; Chan, P.-M.; Cheng, W.-C.; Peng, S.-M.; Lau, K.-C.; Li, W.-K. *J. Am. Chem. Soc.* **2000**, *122*, 11380. (g) Huynh, M. H. V.; Witham, L. M.; Lasker, J. M.; Wetzler, M.; Mort, B.; Jameson, D. L.; White, P. S.; Takeuchi, K. J. *J. Am. Chem. Soc.* **2003**, *125*, 308.

(11) (a) Grover, N.; Thorp, H. H. *J. Am. Chem. Soc.* **1991**, *113*, 7030. (b) Neyhart, G. A.; Grover, N.; Smith, S. R.; Kalsbeck, W. A.; Fairley, T. A.; Cory, M.; Thorp, H. H. *J. Am. Chem. Soc.* **1993**, *115*, 4423. (c) Cheng, C.-C.; Goll, J. G.; Neyhart, G. A.; Welch, T. W.; Singh, P.; Thorp, H. H. *J. Am. Chem. Soc.* **1995**, *117*, 2970. (d) Carter, P. J.; Cheng, C.-C.; Thorp, H. H. *J. Am. Chem. Soc.* **1998**, *120*, 632.

(12) For L = C≡O, see: (a) Thomas, N. C.; Fischer, J. *J. Coord. Chem.* **1990**, *21*, 119. (b) Nagao, H.; Mizukawa, T.; Tanaka, K. *Inorg. Chem.* **1994**, *33*, 3415. (c) Fletcher, N. C.; Keene, F. R. *J. Chem. Soc., Dalton Trans.* **1998**, 2293. For L = $^-$C≡N, see: (d) Belser, P.; von Zelewsky, A.; Juris, A.; Barigelletti, F.; Balzani, V. *Gazz. Chim. Ital.* **1985**, *115*, 723. (e) Yang, J.; Seneviratne, D.; Arbatin, G.; Andersson, A. M.; Curtis, J. C. *J. Am. Chem. Soc.* **1997**, *119*, 5329. For L = $NCCH_3$, see: (f) Hecker, C. R.; Fanwick, P. E.; McMillin, D. R. *Inorg. Chem.* **1991**, *30*, 659. (g) Fagalde, F.; Lis de Katz, N. D.; Katz, N. E. *Polyhedron* **1997**, *16*, 1921.

(13) Takeuchi, K. J.; Thompson, M. S.; Pipes, D. W.; Meyer, T. J. *Inorg. Chem.* **1984**, *23*, 1845.

(14) Demas, J. N.; Crosby, G. A. *J. Phys. Chem.* **1971**, *75*, 991.

Table 1. Crystallography Data

	4$(PF_6)\cdot 2^1/_2CH_3CN$	**5**(PF_6)	**9**$(ClO_4)_2\cdot 2CH_2Cl_2$
chemical formula	$C_{39}H_{33.5}F_6N_{7.5}PRu$	$C_{34}H_{26}F_6N_5OPRu$	$C_{37}H_{35}Cl_6N_5O_{10}Ru$
fw	853.27	766.64	1023.47
cryst size, mm	0.4 × 0.15 × 0.1	0.35 × 0.25 × 0.15	0.4 × 0.2 × 0.15
cryst syst	monoclinic	triclinic	monoclinic
space group	*C*2/*c*	$P\bar{1}$ (no. 2)	$P2_1/c$
a, Å	31.662(6)	8.596(2)	10.453(2)
b, Å	8.807(2)	12.617(3)	11.733(2)
c, Å	27.268(6)	14.961(3)	35.257(7)
α, deg	90	77.98(3)	90
β, deg	95.52(3)	80.13(3)	97.44(3)
γ, deg	90	86.92(3)	90
V, Å^3	7568(3)	1563.3(6)	4287.7(15)
Z	8	2	4
D_c, g cm^{-3}	1.498	1.629	1.585
μ, mm^{-1}	0.526	0.626	0.800
F(000)	3464	772	2072
$2\theta_{max}$, deg	50.6	50.9	50.4
no. indep reflns (R_{int})	4311 (0.063)	4131 (0.051)	4321 (0.042)
no. of obsd data [$I \geq 2\sigma(I)$]	4311	4131	4321
no. of variables	494	434	534
R,[a] R_w[b]	0.051, 0.11	0.061, 0.15	0.034, 0.062

[a] $R = \sum||F_o| - |F_c||/\sum|F_o|$. [b] $R_w = [\sum w(|F_o| - |F_c|)^2/\sum w|F_o|^2]^{1/2}$.

0.05 μm alumina on a microcloth, sonicated for 5 min in deionized water, and rinsed with acetonitrile before use. An $Ag/AgNO_3$ (0.1 M in CH_3CN) electrode was used as reference electrode. All solutions were degassed with argon before experiments. $E_{1/2}$ values are the average of the cathodic and anodic peak potentials for the oxidative and reductive waves. The $E_{1/2}$ value of the ferrocenium/ferrocene couple ($Cp_2Fe^{+/0}$) measured in the same solution was used as an internal reference. All the $E_{1/2}$ values reported in this work and quoted from literature are converted to values versus the $Cp_2Fe^{+/0}$ couple.[15]

Syntheses. [(tpy)(bpy)RuC≡CR](ClO$_4$), 1−8(ClO$_4$). Excess HC≡CR (0.3 mmol) was added to a mixture containing [Ru(tpy)(bpy)(OH_2)]$(ClO_4)_2$ (0.10 g, 0.14 mmol) and Et_3N (1 mL) in acetone (20 mL). After refluxing for 10 h, the solvent was removed under reduced pressure and the crude product was eluted by column chromatography (neutral alumina, 1:3 (v/v) CH_3CN/toluene as eluent) as a purple band. After removal of solvent, the purple solid was washed with diethyl ether and air-dried. This solid was recrystallized by slow diffusion of Et_2O into a CH_3CN solution to give bright violet crystals.

Complex 3(ClO$_4$) (R = Ph): yield 0.068 g, 70%. Anal. Calcd for $C_{33}H_{24}N_5RuClO_4$: C, 57.35; H, 3.50; N, 10.13. Found: C, 56.95; H, 3.56; N, 10.07. ^{1}H NMR (500 MHz, $(CD_3)_2CO$): δ 6.85−6.98 (m, 5H, Ph), 7.21 (t, J_{HH} = 6.5 Hz, 1H, H_m), 7.36 (t, J_{HH} = 6.5 Hz, 1H, H_e), 7.49 (d, J_{HH} = 4.9 Hz, 1H, H_n), 7.86 (d, J_{HH} = 5.0 Hz, 1H, H_f), 7.91 (t, J_{HH} = 7.9 Hz, 1H, H_l), 7.96 (t, J_{HH} = 7.7 Hz, 1H, H_d), 8.01 (t, J_{HH} = 6.6 Hz, 1H, H_h), 8.13 (d, J_{HH} = 8.1 Hz, 1H, H_a), 8.31 (t, J_{HH} = 7.9 Hz, 1H, H_i), 8.57 (d, J_{HH} = 8.0 Hz, 1H, H_c), 8.64 (d, J_{HH} = 8.2 Hz, 1H, H_k), 8.67 (d, J_{HH} = 8.1 Hz, 1H, H_b), 8.83 (d, J_{HH} = 8.1 Hz, 1H, H_j), 10.57 (d, J_{HH} = 5.6 Hz, 1H, H_g). ^{13}C{^{1}H} NMR (126 MHz, $(CD_3)_2CO$): δ 104.3 ($C_α$), 122.3 (C_b), 123.3 (C_k), 123.5 (C_c), 123.9 (C_j), 124.0 (*para* of Ph), 126.6 (C_h), 127.0 (C_m), 127.3 (C_e), 127.8 (*ortho* of Ph), 129.4 (C_{ipso}), 131.3 (*meta* of Ph), 132.4 (C_a), 136.4 (C_d), 136.4 (C_i), 136.9 (C_l), 149.6 (C_n), 151.8 (C_f), 154.5, 154.7 (C_g), 156.3, 156.5, 157.0, 158.4 (quarternary carbons of tpy and bpy), $C_β$ not resolved. IR (cm^{-1}): $\nu_{C≡C}$ 2059, 2068. FAB-MS: *m*/*z* 592 [M$^+$]. For **1**, **2**, and **4**−**8**, see Supporting Information.

[(tpy)(bpy)Ru=C(OMe)(CH$_2$R)](ClO$_4$)$_2$, 9−10(ClO$_4$)$_2$. CF_3COOH (1 mL) was added to a deep violet suspension of [(tpy)(bpy)RuC≡CR](ClO_4) (0.15 mmol) in methanol (5 mL), and this resulted in a change in appearance to a clear orange solution. After stirring for 1 h at room temperature, the solvent was removed under vacuum to leave an oily residue. This was redissolved in MeOH (10 mL), and a saturated aqueous solution of $LiClO_4$ (3 mL) was added. After evaporation of the solvent under vacuum, the orange-red precipitate was washed with water (2 × 5 mL) and recrystallized by slow diffusion of Et_2O into CH_2Cl_2 solution to give bright red crystals. The ^{1}H NMR spectral data are summarized in the Supporting Information.

Complex 9(ClO$_4$)$_2$ (R = C$_6$H$_4$OMe-4): yield 0.10 g, 80%. Anal. Calcd for $C_{35}H_{30}N_5RuCl_3O_{10}\cdot 0.7CH_2Cl_2$: C, 45.25; H, 3.34; N, 7.39. Found: C, 45.20; H, 3.52; N, 7.09. ^{13}C{^{1}H} NMR (126 MHz, CD_2Cl_2): δ 51.3 (CH_2); 55.5 (OMe of Ar); 64.5 (=C−O*Me*); 114.7, 119.8, 123.2, 123.6, 124.1, 124.2, 127.4, 128.1, 128.4, 128.5, 138.5, 138.9, 139.1, 142.1, 147.6, 152.9, 153.5, 154.9, 155.5, 156.5, 157.1, 158.8; 317.7 (Ru=C). FAB-MS: *m*/*z* 654 [M$^+$].

Complex 10(ClO$_4$)$_2$ (R = *t*-Bu): yield 0.09 g, 71%. Anal. Calcd for $C_{32}H_{33}N_5RuCl_2O_9\cdot 0.3CH_2Cl_2$: C, 46.79; H, 4.08; N, 8.45. Found: C, 46.94; H, 4.05; N, 8.46. ^{13}C{^{1}H} NMR (126 MHz, CD_2Cl_2): δ 30.5 (C*Me*$_3$); 33.8 (*C*Me$_3$); 62.7 (CH_2); 66.1 (OMe); 123.6, 123.8, 124.4, 125.0, 125.2, 127.9, 128.5, 128.7, 137.4, 139.1, 139.2, 139.6, 147.7, 153.5, 153.9, 154.0, 156.3, 157.0, 157.4; 328.9 (Ru=C). FAB-MS: *m*/*z* 624 [M$^+$].

Photochemical Reaction. Complex **9**$(ClO_4)_2$ (0.05 g) was dissolved in CH_3CN (2 mL), transferred into a sealed quartz cell, and three freeze−pump−thaw cycles were performed. The sample was placed into a RPR-100 Rayonet photochemical chamber reactor equipped with 16 8-W RPR 3500 Å Hg lamps and irradiated for 12 h. Et_2O (10 mL) was then added to precipitate any inorganic salt. The remaining solution was filtered through an alumina column and concentrated. The inorganic salt precipitated was characterized using ^{1}H NMR and FAB-MS, and the organic product was identified by ^{1}H NMR and GC−MS. Photolysis of **10**$(ClO_4)_2$ in CH_2Cl_2 was similarly performed.

X-ray Crystallography. The crystal data and details of data collection and refinement for **4**$(PF_6)\cdot 2^1/_2CH_3CN$, **5**(PF_6), and **9**$(ClO_4)_2\cdot 2CH_2Cl_2$ are summarized in Table 1. A MAR diffractometer with a 300 mm image plate detector using graphite-monochromatized Mo Kα radiation (λ = 0.71073 Å) was employed for data collection at 253(2) K. The images were interpreted and intensities integrated using the program DENZO,[16] and structures were solved by direct methods

(15) Connelly, N. G.; Geiger, W. E. *Chem. Rev.* **1996**, *96*, 877.

(16) *DENZO*: In *The HKL Manual, A description of programs DENZO, XDISPLAYF and SCALEPACK*; written by Gewirth, D. with the cooperation of the program authors Otwinowski, Z.; and Minor, W. Yale University: New Haven, CT, 1995.

employing the SIR-97 program[17] on a PC. The Ru, P, Cl, and many non-H atoms were located according to the direct methods. The positions of the other non-hydrogen atoms were found after successful refinement by full-matrix least-squares using the program SHELXL-97 on a PC.[18] Except for disordered atoms, non-hydrogen atoms were refined anisotropically in the final stage of least-squares refinement. Unless otherwise stated, the positions of the H atoms were calculated on the basis of the riding mode with thermal parameters equal to 1.2 times that of the associated C atom. For **4**$(PF_6)\cdot 2^1/_2CH_3CN$, one formula unit was located in the asymmetric unit. Disorder is observed in the PF_6^- anion, and some restraints had been applied. For both **5**(PF_6) and **9**$(ClO_4)_2\cdot 2CH_2Cl_2$, one crystallographic asymmetric unit consists of one formula unit.

Results

Syntheses and Characterization. In the literature, accounts of the preparation of acetylide- and alkoxycarbene-ruthenium complexes supported by phosphine and cyclopentadienyl/arene ligands are extensive,[19] while congeners bearing N-donor auxiliaries have also been described.[20] We recently reported on arylacetylideruthenium(II) complexes supported by macrocyclic N-donor ligands, namely, [Ru(Me_3tacn)(PMe_3)$_2$(C≡CAr)]-PF_6 (Me_3tacn = 1,4,7-trimethyl-1,4,7-triazacyclononane)[21] and *trans*-[Ru(16-TMC)(C≡CAr)$_2$] (16-TMC = 1,5,9,13-tetramethyl-1,5,9,13-tetraazacyclohexadecane).[22] In this work, we have synthesized acetylide-, and methoxycarbene-ruthenium complexes containing only polypyridyl ligands. Reaction of the aqua complex [(tpy)(bpy)Ru-$(OH_2)]^{2+}$ with HC≡CR in the presence of Et_3N in refluxing acetone afforded the acetylide complexes $[(tpy)(bpy)RuC{\equiv}CR]^+$ (Scheme 1) with overall yields of around 70%. Purification by column chromatography (neutral alumina, 1:3 (v/v) CH_3CN/toluene as eluent) prior to recrystallization (slow diffusion of Et_2O into a CH_3CN solution) was needed to obtain analytically pure $[(tpy)(bpy)RuC{\equiv}CR]^+$ salts. The desired product $[(tpy)(bpy)RuC{\equiv}CR]^+$ was eluted as a purple band, followed by an orange band, which was characterized as $[(tpy)(bpy)Ru(N{\equiv}CCH_3)]^{2+}$.[12f] We have attempted to improve the product yield by varying the amount of HC≡CR and Et_3N, but no significant improvement was found. The acetylide complexes **1**−**8** are sufficiently stable to be handled in air under ambient conditions in solution and solid forms. For example, the UV−visible spectrum of **3** remains unchanged in CH_3CN or CH_2Cl_2 after 5 days.

Scheme 1

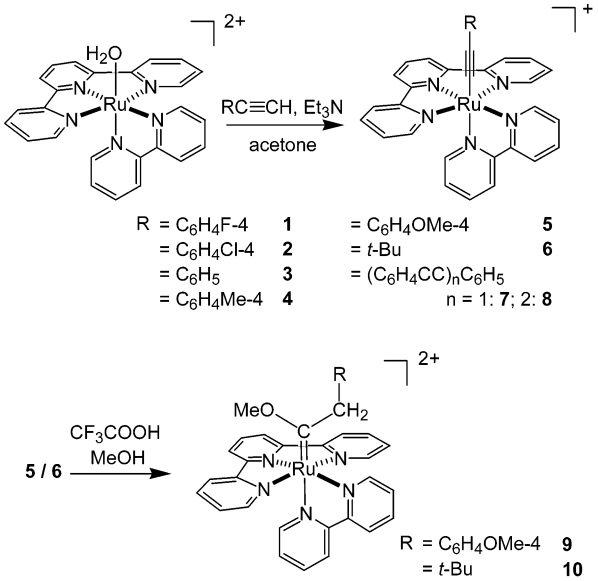

The acetylide complexes have been characterized by various spectroscopic means. Their IR spectra show stretching frequencies at 2050−2070 cm^{-1}, which are attributed to the ν(C≡C) stretching of the coordinated acetylide ligand. It is interesting to note that the $\nu_{C\equiv C}$ frequencies of $[(tpy)(bpy)RuC{\equiv}CR]^+$ are higher than those of *trans*-[Ru(16-TMC)(C≡CAr)$_2$] [22a] ($\nu_{C\equiv C}$ 2002−2012 cm^{-1}), which are supported by a purely σ-donating macrocyclic amine ligand. The ^{1}H NMR signals for the polypyridyl ligands (see Figure 1 for the labeling scheme) have been unambiguously assigned using ^{1}H−^{1}H COSY and ^{1}H−^{1}H NOESY NMR techniques (see Supporting Information). The ^{1}H−^{1}H COSY technique gives information on through-bond coupling, and thus associated protons on each pyridyl ring can be distinguished. The through-space relationships of H_b−H_c and H_j−H_k are revealed by the ^{1}H−^{1}H NOESY technique, while the NOE response between H_f and H_g signifies that the pyridyl group containing H_{g-j} is *trans* to the central tpy ring, while the pyridyl group with H_{k-n} is *trans* to the acetylide ligand. The aromatic ^{1}H signals

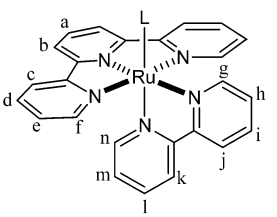

Figure 1. Labeling scheme for hydrogen and carbon atoms in complexes **1**−**10**.

(17) SIR-97: Altomare, A.; Burla, M. C.; Camalli, M.; Cascarano, G.; Giacovazzo, C.; Guagliardi, A.; Moliterni, A. G. G.; Polidori, G.; Spagna, R. *J. Appl. Crystallogr.* **1998**, *32*, 115.

(18) Sheldrick, G. M. *SHELXL-97*, Programs for Crystal Structure Analysis (release 97−2); University of Goetingen: Germany, 1997.

(19) For example, see: (a) Bozec, H. L.; Ouzzine, K.; Dixneuf, P. H. *Organometallics* **1991**, *10*, 2768. (b) Pilette, D.; Ouzzine, K.; Bozec, H. L.; Dixneuf, P. H.; Rickard, C. E. F.; Roper, W. R. *Organometallics* **1992**, *11*, 809. (c) Uno, M.; Dixneuf, P. H. *Angew. Chem., Int. Ed.* **1998**, *37*, 1714. (d) Colbert, M. C. B.; Lewis, J.; Long, N. J.; Raithby, P. R.; Younus, M.; White, A. J. P.; Williams, D. J.; Payne, N. N.; Yellowlees, L.; Beljonne, D.; Chawdhury, N.; Friend, R. H. *Organometallics* **1998**, *17*, 3034. (e) McDonagh, A. M.; Humphrey, M. G.; Samoc, M.; Luther-Davies, B.; Houbrechts, S.; Wada, T.; Sasabe, H.; Persoons, A. *J. Am. Chem. Soc.* **1999**, *121*, 1405. (f) Bruce, M. I.; Low, P. J.; Costuas, K.; Halet, J.-F.; Best, S. P.; Heath, G. A. *J. Am. Chem. Soc.* **2000**, *122*, 1949. (g) Rigaut, S.; Monnier, F.; Mousset, F.; Touchard, D.; Dixneuf, P. H. *Organometallics* **2002**, *21*, 2654. (h) Powell, C. E.; Cifuentes, M. P.; Morrall, J. P.; Stranger, R.; Humphrey, M. G.; Samoc, M.; Luther-Davies, B.; Heath, G. A. *J. Am. Chem. Soc.* **2003**, *125*, 602. (i) Long, N. J.; Williams, C. K. *Angew. Chem., Int. Ed.* **2003**, *42*, 2586.

(20) (a) Yam, V. W.-W.; Chu, B. W.-K.; Cheung, K.-K. *Chem. Commun.* **1998**, 2261. (b) Slugovc, C.; Mereiter, K.; Schmid, R.; Kirchner, K. *Organometallics* **1998**, *17*, 827. (c) Rüba, E.; Gemel, C.; Slugovc, C.; Mereiter, K.; Schmid, R.; Kirchner, K. *Organometallics* **1999**, *18*, 2275. (d) Cadierno, V.; Gamasa, M. P.; Gimeno, J.; Iglesias, L.; García-Granda, S. *Inorg. Chem.* **1999**, *38*, 2874. (e) Tenorio, M. A. J.; Tenorio, M. J.; Puerta, M. C.; Valerga, P. *Organometallics* **2000**, *19*, 1333. (f) Bianchini, C.; Lee, H. M. *Organometallics* **2000**, *19*, 1833. (g) Menéndez, C.; Morales, D.; Pérez, J.; Riera, V.; Miguel, D. *Organometallics* **2001**, *20*, 2775. (h) Rüba, E.; Hummel, A.; Mereiter, K.; Schmid, R.; Kirchner, K. *Organometallics* **2002**, *21*, 4955.

(21) Yang, S.-M.; Chan, M. C.-W.; Cheung, K.-K.; Che, C.-M.; Peng, S.-M. *Organometallics* **1997**, *16*, 2819.

(22) (a) Choi, M.-Y.; Chan, M. C.-W.; Zhang, S.; Cheung, K.-K.; Che, C.-M.; Wong, K.-Y. *Organometallics* **1999**, *18*, 2074. (b) Choi, M.-Y.; Chan, M. C. W.; Peng, S.-M.; Cheung, K.-K.; Che, C.-M. *Chem. Commun.* **2000**, 1259.

of the arylacetylide group appear at 6.54−7.60 ppm, and the *t*-Bu group for complex **6** is observed at 0.82 ppm.

The carbene-ruthenium complexes $[(tpy)(bpy)Ru{=}C(OMe)(CH_2R)]^{2+}$ (R = C_6H_4OMe (**9**), *t*-Bu (**10**)) were synthesized by treatment of the corresponding acetylide complexes $[(tpy)(bpy)RuC{\equiv}CR]^+$ with MeOH under acidic conditions. Hence addition of CF_3COOH or HCl gas into the reaction mixture yielded the carbene complexes. However, prolonged bubbling of HCl gas (over 1 h) gave $[(tpy)(bpy)RuCl](ClO_4)$ as the major product. Similarly, the same procedure can be adopted using EtOH to synthesize the ethoxycarbene derivatives $[(tpy)(bpy)Ru{=}C(OEt)(CH_2R)]^{2+}$.[23] The carbene complexes are stable as solids under air, but they are unstable in solution. For example, the use of a CH_3CN/Et_2O mixture for recrystallization of **9** afforded $[(tpy)(bpy)Ru(N{\equiv}CCH_3)](ClO_4)_2$ as the major product. Deaerated acetone-d_6 was used for NMR studies on the carbene complexes, but changes in the spectra were detected after 5 h. After careful consideration of the stability and solubility of the ruthenium carbene complexes in this work, CH_2Cl_2 was selected as the solvent of choice; complexes **9** and **10** remain unchanged in CH_2Cl_2 solutions at room temperature *in the dark* for at least 5 days (by UV−vis and ^1H NMR spectroscopy), although they are transformed into $[(tpy)(bpy)RuCl]^+$ in refluxing CH_2Cl_2. Indeed, we have found that complexes **9** and **10** are unstable in CH_2Cl_2 and CH_3CN solutions at room temperature under ambient light (changes in their UV−vis and ^1H NMR spectra are detectable after 1 day) and when irradiated with UV−visible light (see Photochemistry section).

Complexes **9** and **10** show low-field ^{13}C NMR signals at 317.7 and 328.9 ppm, respectively, which are characteristic for the carbene carbon atom,[19a,b,24] and the ^1H signals at 4.43 and 4.39 ppm (s, 3H) respectively confirm the presence of the −OMe group on the carbene carbon. Upon comparing the corresponding ^1H signals of the polypyridyl ligands for the acetylide and carbene complexes (**5** vs **9**; **6** vs **10**), it was found that all of them gave very similar chemical shifts in CD_2Cl_2 (differences less than 0.2 ppm) except for H_g, which appears for **5** and **6** at 10.51 and 10.55 ppm, respectively, and for **9** and **10** at 9.34 and 8.86 ppm, respectively. In addition, the ^1H shift of H_g for $[(tpy)(bpy)Ru(N{\equiv}CCH_3)]^{2+}$ appears at 9.75 ppm in CD_2Cl_2. The highly sensitive nature of the chemical shift for H_g as the ligand changes from acetonitrile to acetylide and carbene is consistent with their proximity to each other; H_g is the only proton among the polypyridine rings that protrudes above the tpy plane and toward these ligands.

Since the insertion of carbene groups into C=C bonds mediated by carbene-ruthenium complexes is of great current interest,[25,26] we have examined the reactions of complexes **9** and **10** with styrene. For example, excess styrene (10 equiv) was added to a CH_2Cl_2 solution (10 mL) of **10** (0.1 mmol), and this was stirred at room temperature in the dark and monitored by UV−visible spectroscopy. However, no observable change in the spectrum and no reaction was found after 48 h.

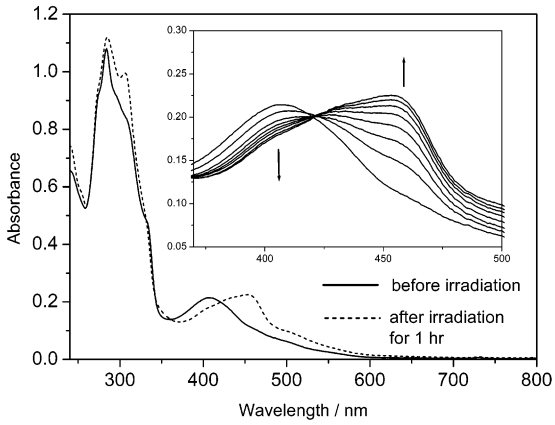

Figure 2. UV−visible spectral trace for **10** in CH_3CN during photolysis. The inset shows the time trace at 2 min intervals.

Photochemistry. The carbene complexes **9** and **10** are unstable in solution upon strong irradiation. Preliminary photolyses of **9** in CH_2Cl_2 and **10** in CH_3CN were performed by irradiating samples with UV−visible light using Hg air lamps for 5 h in a photochemical reaction chamber. Figure 2 shows the time trace of the UV−visible spectra for **10** in CH_3CN during the photolysis reaction; no further spectral changes were observed after 1 h, and the reactions were clearly complete. The metal-organic products were precipitated by adding Et_2O to the CH_2Cl_2 and CH_3CN solutions, and the isolated salts were characterized as $[(tpy)(bpy)RuCl]^+$ and $[(tpy)(bpy)Ru(NCCH_3)]^{2+}$, respectively, using ^1H NMR and FAB-MS techniques.

A detailed investigation on the photochemical reactivity of **9** in CH_3CN was performed. Complex **9**$(ClO_4)_2$ in degassed CH_3CN was irradiated by UV−visible light in the photochemical reaction chamber for 12 h, after which Et_2O was added to the resultant mixture to precipitate $[(tpy)(bpy)RuN{\equiv}CCH_3](ClO_4)_2$ (characterized by ^1H NMR and FAB-MS). To characterize the organic product(s), the remaining solution was passed through a short alumina column, concentrated, and analyzed by ^1H and GC−MS; the major product and indeed the only identifiable compound was 4-methoxybenzaldehyde.

Crystal Structures. The structures of **4**(PF_6), **5**(PF_6), and **9**$(ClO_4)_2$ have been determined by X-ray crystal-

(23) Characterization data for $[(tpy)(bpy)Ru{=}C(OEt)(CH_2C_6H_4OMe)](ClO_4)_2$: ^1H NMR (400 MHz, (CD_2Cl_2): δ 1.29 (t, $^3J_{HH}$ = 7.5 Hz, 3H, OCH_2CH_3), 3.69 (s, 3H, OMe), 4.23 (s, 2H, $CH_2C_6H_4OMe$), 4.62 (q, $^3J_{HH}$ = 7.0 Hz, 2H, OCH_2CH_3), 5.98 (d, $^3J_{HH}$ = 8.7 Hz, 2H, Ar), 6.44 (d, $^3J_{HH}$ = 8.7 Hz, 2H, Ar), 7.08 (d, J_{HH} = 5.3 Hz, 1H, H_n), 7.25 (t, J_{HH} = 6.5 Hz, 1H, H_m), 7.34 (t, J_{HH} = 6.6 Hz, 1H, H_e), 7.71 (d, J_{HH} = 5.5 Hz, 1H, H_f), 7.86−7.92 (m, 2H, H_d and H_l), 7.99 (t, J_{HH} = 6.7 Hz, 1H, H_k), 8.14 (d, J_{HH} = 7.8 Hz, 1H, H_c), 8.17 (t, J_{HH} = 8.2 Hz, 1H, H_a), 8.22−8.26 (m, 2H, H_b and H_i), 8.50 (d, J_{HH} = 7.6 Hz, 1H, H_j), 9.26 (d, J_{HH} = 5.6 Hz, 1H, H_g). FAB-MS: *m/z* 669 $[M^+]$.

(24) (a) Ruiz, N.; Péron, D.; Dixneuf, P. H. *Organometallics* **1995**, *14*, 1095. (b) Štěpnička, P.; Gyepes, R.; Lavastre, O.; Dixneuf, P. H. *Organometallics* **1997**, *16*, 5089.

(25) (a) Doyle, M. P.; Forbes, D. C. *Chem. Rev.* **1998**, *98*, 911. (b) Naota, T.; Takaya, H.; Murahashi, S.-I. *Chem. Rev.* **1998**, *98*, 2599. (c) Trost, B. M.; Toste, F. D.; Pinkerton, A. B. *Chem. Rev.* **2001**, *101*, 2067.

(26) (a) Nishiyama, H.; Itoh, Y.; Matsumoto, H.; Park, S.-B.; Itoh, K. *J. Am. Chem. Soc.* **1994**, *116*, 2223. (b) Park, S.-B.; Sakata, N.; Nishiyama, H. *Chem. Eur. J.* **1996**, *2*, 303. (c) Lee, H. M.; Bianchini, C.; Jia, G.; Barbaro, P. *Organometallics* **1999**, *18*, 1961. (d) Galardon, E.; Maux, P. L.; Simonneaux, G. *Tetrahedron* **2000**, *56*, 615. (e) Munslow, I. J.; Gillespie, K. M.; Deeth, R. J.; Scott, P. *Chem. Commun.* **2001**, 1638. (f) Che, C.-M.; Huang, J.-S.; Lee, F.-W.; Li, Y.; Lai, T.-S.; Kwong, H.-L.; Teng, P.-F.; Lee, W.-S.; Lo, W.-C.; Peng, S.-M.; Zhou, Z.-Y. *J. Am. Chem. Soc.* **2001**, *123*, 4119. (g) Li, Y.; Huang, J.-S.; Zhou, Z.-Y.; Che, C.-M. *J. Am. Chem. Soc.* **2001**, *123*, 4843. (h) Miller, J. A.; Jin, W.; Nguyen, S. T. *Angew. Chem., Int. Ed.* **2002**, *41*, 2953. (i) Li, Y.; Huang, J.-S.; Zhou, Z.-Y.; Che, C.-M.; You, X.-Z. *J. Am. Chem. Soc.* **2002**, *124*, 13185.

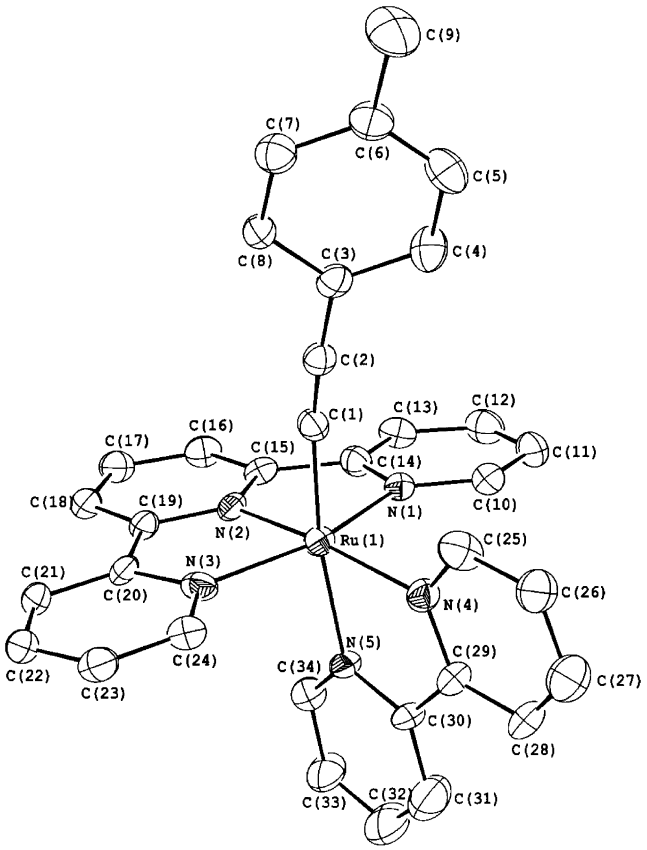

Figure 3. Perspective view of the cation in **4** (30% probability ellipsoids).

lography. Perspective views of the complex cations of **4** and **9** are shown in Figures 3 and 4, respectively. Relevant bond lengths and angles are listed in Table 2. In each case, the Ru atom adopts a distorted octahedral geometry. The Ru−C(1) [**4**, 2.025(9); **5**, 2.025(7) Å] and C(1)−C(2) distances [**4**, 1.192(10); **5**, 1.191(9) Å] are comparable to previously reported Ru(II) acetylide complexes (Ru−C_α = 1.91−2.12 Å, C_α−C_β = 1.13−1.22 Å).[27] The short Ru−C(1) distance in **9** [1.933(6) Å], together with the angles around the C(1) atom (which are consistent with sp^2 hybridization), indicate the presence of ruthenium−carbon multiple bonding, presumably via Ru(II) → π^*(carbene) π-back-bonding interactions. The C(1)−C(2) and C(1)−O(1) distances [1.529(7) and 1.305(6) Å, respectively] in **9** demonstrate their single-bonded nature.

Table 2. Selected Bond Length (Å) and Angles (deg)

	4	**5**	**9**
Ru−C(1)	2.025(9)	2.025(7)	1.933(6)
C(1)−C(2)	1.192(10)	1.191(9)	1.529(7)
Ru−N(1)	2.047(5)	2.081(6)	2.054(4)
Ru−N(2)	1.948(5)	1.961(5)	1.965(4)
Ru−N(3)	2.065(6)	2.054(6)	2.073(5)
Ru−N(4)	2.127(6)	2.102(6)	2.104(4)
Ru−N(5)	2.100(7)	2.128(5)	2.177(4)
C(1)−O(1)			1.305(6)
Ru−C(1)−C(2)	170.7(7)	170.8(6)	126.3(5)
C(1)−Ru−N(1)	92.0(3)	91.3(2)	93.8(2)
C(1)−Ru−N(2)	95.4(3)	90.5(3)	94.8(2)
C(1)−Ru−N(3)	91.2(3)	92.3(2)	87.6(2)
C(1)−Ru−N(4)	91.8(3)	92.0(2)	96.3(2)
C(1)−Ru−N(5)	168.8(3)	167.6(2)	171.9(2)
Ru−C(1)−O(1)			116.1(4)

Electrochemistry. Cyclic voltammetry was used to examine the electrochemistry of complexes **1**−**10** (Table 3; all values vs $Cp_2Fe^{+/0}$). Complexes **1**−**8** show two reversible/quasi-reversible couples at $E_{1/2}$ = −2.22 to −2.14 and −1.95 to −1.87 V, and an irreversible wave at E_{pa} = 0.15 to 0.26 V (scan rate = 50 mV s^{-1}, 0.1 M $[Bu_4N]PF_6$ in CH_3CN as supporting electrolyte; the latter wave is irreversible even at scan rates of up to 1000 mV s^{-1}). The span in the E_{pa} values for the irreversible wave from R = C_6H_4F-4 (**1**) to C_6H_4OMe-4 (**5**) is 110 mV. The electrochemistry of **7** was also examined in CH_2Cl_2 solution (0.1 M $[Bu_4N]PF_6$ as supporting electrolyte), and very similar results were observed, namely, a quasi-reversible couple at $E_{1/2}$ = −1.94 V and an irreversible wave at E_{pa} = 0.26 V.

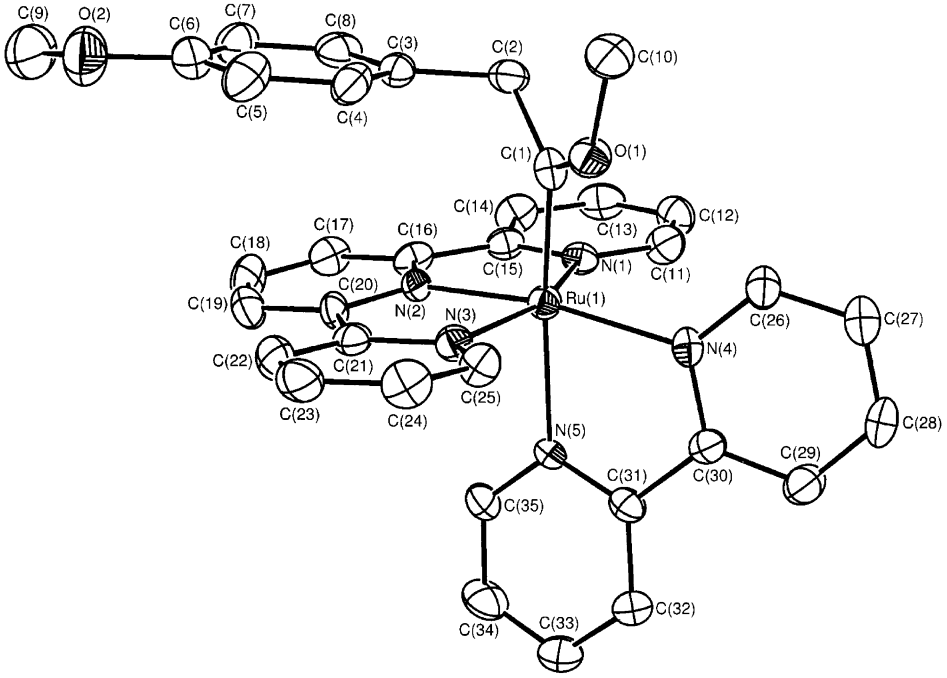

Figure 4. Perspective view of the cation in **9** (30% probability ellipsoids).

Table 3. Electrochemical Data for [(tpy)(bpy)RuC≡CR]ClO_4 (1−8)[a] and [(tpy)(bpy)Ru=C(OMe)(CH_2R)](ClO_4)$_2$ (9 and 10)[b]

complex	$E_{1/2}$[c]/V vs $Cp_2Fe^{+/0}$		
1 (R = C_6H_4F-4)	−2.15	−1.90	0.26[d]
2 (R = C_6H_4Cl-4)	−2.16	−1.89	0.26[d]
3 (R = Ph)	−2.16	−1.89	0.24[d]
4 (R = C_6H_4Me-4)	−2.17	−1.90	0.20[d]
5 (R = C_6H_4OMe-4)	−2.17	−1.90	0.15[d]
6 (R = *t*-Bu)	−2.22	−1.95	0.18[d]
7 (R = C_6H_4C≡CPh)	−2.16	−1.88	0.25[d]
8 (R = $(C_6H_4C{\equiv}C)_2$Ph)	−2.14	−1.87	0.26[d]
9 (R = C_6H_4OMe-4)	−2.03	−1.57	0.99
10 (R = *t*-Bu)	−2.04	−1.50	1.00

[a] Supporting electrolyte: 0.1 M [Bu_4N]PF_6 in CH_3CN. [b] Supporting electrolyte: 0.1 M [Bu_4N]PF_6 in CH_2Cl_2. [c] $E_{1/2} = (E_{pc} + E_{pa})/2$ at 25 °C for reversible couples. [d] Irreversible; the recorded potential is the anodic peak potential at a scan rate of 50 mV s^{-1}.

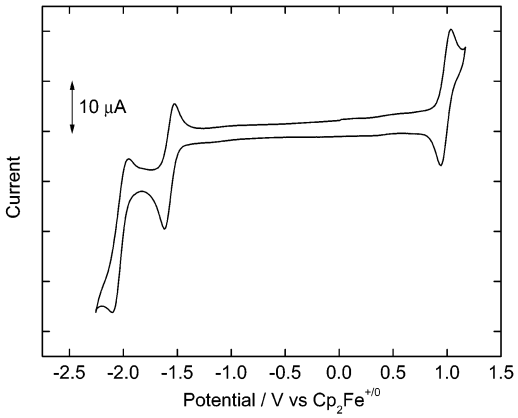

Figure 5. Cyclic voltammogram for **9** in CH_2Cl_2 with [*n*Bu_4N]PF_6 (0.1 M) as supporting electrolyte. Conditions: working electrode, glassy-carbon; scan rate, 50 mV s^{-1}.

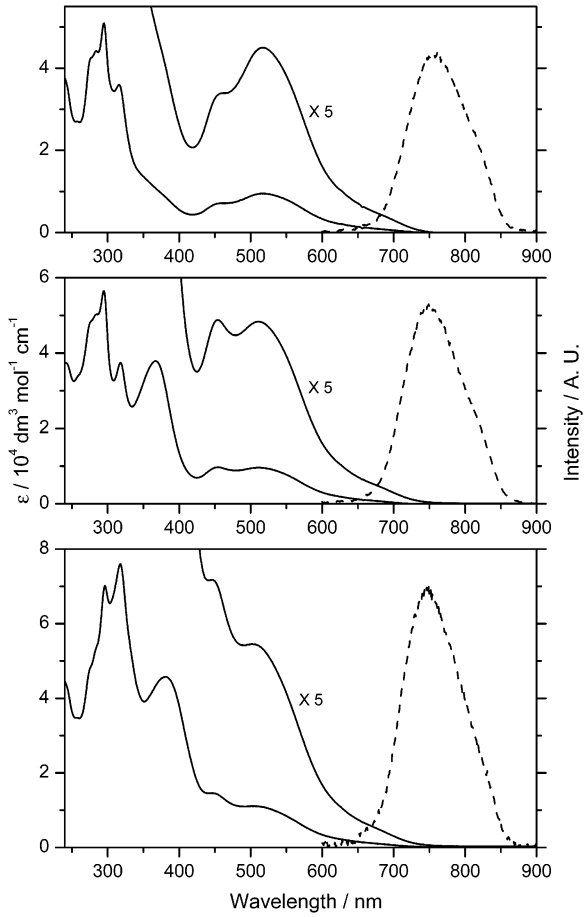

Figure 6. Absorption (—, CH_3CN, 298 K) and emission (- - -, CH_3CN, 298 K, λ_{ex} = 550 nm, complex concentration = 1 × 10^{-4} M) spectra of [(tpy)(bpy)Ru($C{\equiv}CC_6H_4)_nC{\equiv}$CPh]$^+$ [*n* = 0 (**3**, top), 1 (**7**, middle), and 2 (**8**, bottom)].

Complexes **9** and **10** show three reversible/quasi-reversible couples at $E_{1/2}$ = −2.03 and −2.04, −1.57 and −1.50, and 0.99 and 1.00 V, respectively, and the cyclic voltammogram for **9** is depicted in Figure 5.

Electronic Spectroscopy. The UV−visible spectral data of [(tpy)(bpy)RuC≡CR]ClO_4 (**1**−**8**) and [(tpy)(bpy)-Ru=C(OMe)(CH_2R)](ClO_4)$_2$ (**9** and **10**) are summarized in Table 4. The absorption spectra of **3**, **7**, and **8** (in CH_3-CN) are depicted in Figure 6. Complexes **1**−**6** exhibit intense high-energy bands at $\lambda_{max} \leq 400$ nm ($\epsilon_{max} \geq 10^4$ dm^3 mol^{-1} cm^{-1}) and a moderately intense band at λ_{max} = 513−526 nm (ϵ_{max} = (9−10) × 10^3 dm^3 mol^{-1} cm^{-1}) with a shoulder around 456−463 nm (ϵ_{max} = (6−7) × 10^3 dm^3 mol^{-1} cm^{-1}). The absorption maxima, especially for the low-energy bands, are affected by the nature of the solvent: for **3**, the absorption peak maxima at 295, 316, 367, and 516 nm in CH_3CN shift to 296, 317, 360, and 524 nm in CH_2Cl_2, respectively. The impact of the *para* substituent on the arylacetylide ligand upon the profile of the absorption band in the visible region is not dramatic. The peak maximum slightly red-shifts in energy as the electron-donating ability of the *para* substituent in R = C_6H_4X-4 increases, except for X = F [λ_{max} = 513 nm for **2** (X = Cl), 516 nm for **1** (F), ∼516 nm for **3** (H), 518 nm for **4** (Me), 520 nm for **5** (OMe)], and they are all blue-shifted with respect to **6** (R = *t*-Bu, λ_{max} = 526 nm). The range of λ_{max} values for **1**−**6** is small, and the energy difference between **2** (513 nm) and **6** (526 nm) is 482 cm^{-1}. Complexes **7** and **8** display intense absorption bands with peak maxima at 367 and 381 nm, respectively (ϵ_{max} = (3−5) × 10^4 dm^3 mol^{-1} cm^{-1}), plus bands in the visible region at λ_{max} = 454 and 513 nm for **7** and 446 and 502 nm for **8** (all $\epsilon_{max} \approx$

Table 4. UV−Visible Absorption Data for [(tpy)(bpy)RuC≡CR]ClO_4 (1−8) in CH_3CN and [(tpy)(bpy)Ru=C(OMe)(CH_2R)](ClO_4)$_2$ (9 and 10) in CH_2Cl_2

complex	absorption λ_{abs}/nm (ϵ/dm^3 mol^{-1} cm^{-1})
1 (R = C_6H_4F-4)	283 (sh) (39 550), 294 (44 460), 316 (31 100), 370 (sh) (8790), 457 (sh) (6310), 516 (8570), 681 (sh) (870)
2 (R = C_6H_4Cl-4)	284 (sh) (38 410), 295 (46 230), 316 (36 500), 361 (sh) (12 860), 456 (sh) (6860), 513 (8750), 681 (sh) (810)
3 (R = Ph)	284 (sh) (44 180), 295 (50 940), 316 (35 950), 367 (sh) (12 430), 456 (sh) (6750), 516 (8990), 682 (sh) (840)
4 (R = C_6H_4Me-4)	283 (sh) (42 300), 295 (47 700), 316 (34 330), 363 (sh) (10 700), 456 (sh) (6460), 518 (8600), 680 (sh) (970)
5 (R = C_6H_4OMe-4)	282 (sh) (44 330), 295 (47 090), 317 (33 660), 364 (sh) (10 860), 459 (sh) (6480), 520 (8500), 680 (sh) (1060)
6 (R = *t*-Bu)	276 (sh) (42 850), 295 (47 770), 315 (29 020), 362 (sh) (9700), 463 (sh) (6350), 526 (10 250), 684 (sh) (1300)
7 (R = C_6H_4C≡CPh)	278 (sh) (48 650), 295 (56 490), 318 (37 480), 367 (37 890), 454 (9690), 513 (9580), 686 (sh) (590)
8 (R = $(C_6H_4C{\equiv}C)_2$Ph)	278 (sh) (49 150), 296 (70 150), 318 (75 930), 381 (45 740), 446 (14 580), 502 (11 060), 683 (sh) (930)
9 (R = C_6H_4OMe-4)	230 (29 650), 285 (42 220), 310 (34 030), 335 (sh) (16 380), 415 (8620), 515 (sh) (1670)
10 (R = *t*-Bu)	242 (36 040), 285 (62 940), 312 (sh) (47 800), 334 (sh) (28 670), 408 (13 350), 503 (sh) (3570)

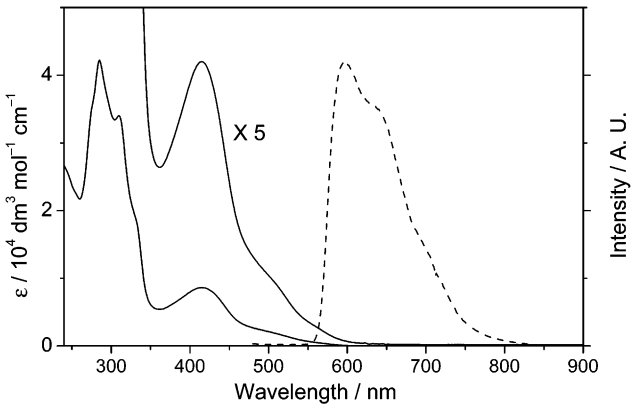

Figure 7. Absorption (—, CH_3CN, 298 K) and glass emission (- - -, *n*-butyronitrile, 77 K, $\lambda_{ex} = 415$ nm, complex concentration $= 1 \times 10^{-4}$ M) spectra of **9**.

Table 5. Emission Data for [(tpy)(bpy)RuC≡CR]ClO_4 (1−8) and [(tpy)(bpy)Ru=C(OMe)(CH_2R)]$(ClO_4)_2$ (9 and 10)[a]

fluid solution (2.5×10^{-5} M)	298 K:[b,c] λ_{max}/nm; Φ	77 K:[d] λ_{max}/nm; τ/μs
1 (R = C_6H_4F-4)	752; 2.1×10^{-4}	721; 1.1
2 (R = C_6H_4Cl-4)	750; 3.2×10^{-4}	723; 1.1
3 (R = Ph)	758; 2.3×10^{-4}	720; 1.3
4 (R = C_6H_4Me-4)	765; 1.2×10^{-4}	718; 1.0
5 (R = C_6H_4OMe-4)	775; 0.4×10^{-4}	733; 0.7
6 (R = *t*-Bu)	786; 0.9×10^{-4}	722; 1.2
7 (R = $C_6H_4C{\equiv}CPh$)	749; 4.4×10^{-4}	728; 1.5
8 (R = $(C_6H_4C{\equiv}C)_2Ph$)	748; 3.6×10^{-4}	725; 1.3
9 (R = C_6H_4OMe-4)	nonemissive	597; 8.3
10 (R = *t*-Bu)	nonemissive	615; 3.9

solid state	298 K:[c] λ_{max}/nm	77 K:[c] λ_{max}/nm
1 (R = C_6H_4F-4)	770	738
2 (R = C_6H_4Cl-4)	752	747
3 (R = Ph)	745	741
4 (R = C_6H_4Me-4)	765	755
5 (R = C_6H_4OMe-4)	776	767
6 (R = *t*-Bu)	780	780
7 (R = $C_6H_4C{\equiv}CPh$)	742	749
8 (R = $(C_6H_4C{\equiv}C)_2Ph$)	746	745
9 (R = C_6H_4OMe-4)	649	616
10 (R = *t*-Bu)	711	630

[a] $\lambda_{ex} = 550$ nm for **1**−**8** and 415 nm for **9** and **10**. [b]Measured in acetonitrile for **1**−**8** and in CH_2Cl_2 for **9** and **10** at 298 K. [c]Lifetimes of ≤0.1 μs were detected for all complexes in the solid state and at 298 K in solution. [d]Measured in MeOH/EtOH (1/4 v/v) for **1**−**8** and in *n*-butyronitrile for **9** and **10**.

1×10^4 dm^3 mol^{-1} cm^{-1}) that are similar to **1**−**6**. It should be noted that the absorption profile and extinction coefficients of the absorption bands for **8** at $\lambda =$ 280−350 nm are different from those for **1**−**7**. The absorption spectrum of **9** in CH_2Cl_2 is depicted in Figure 7. The spectra of **9** and **10** show intense high-energy bands at $\lambda_{max} \leq 350$ nm ($\epsilon_{max} \geq 10^4$ dm^3 mol^{-1} cm^{-1}) and a moderately intense band at $\lambda_{max} = 415$ and 408 nm ($\epsilon_{max} = (8-10) \times 10^3$ dm^3 mol^{-1} cm^{-1}) with a shoulder near 515 and 503 nm ($\epsilon_{max} = (2-4) \times 10^3$ dm^3 mol^{-1} cm^{-1}), respectively.

Emission Spectroscopy. The emission properties of the complexes are summarized in Table 5. Complexes **1**−**8** are emissive in CH_3CN (298 K) and glassy MeOH/EtOH (1/4, v/v; 77 K) solutions and in the solid state (298 and 77 K). Excitation of **1**−**8** at $\lambda = 550$ nm in CH_3CN at 298 K gave a red emission at $\lambda_{max} = 748-786$ nm with short lifetimes (≤0.1 μs) and very low quantum yields (ca. 10^{-4}). The emission of **3** was also examined in CH_2Cl_2 solution, and the luminescent properties are similar to those found in CH_3CN (see Supporting Information). For **1**−**5**, the emission maximum slightly red-shifts in energy as the electron-donating ability of the substituent on C_6H_4X-4 increases, except for X = F [$\lambda_{max} = 750$ nm for **2** (X = Cl), 752 nm for **1** (F), 758 nm for **3** (H), 765 nm for **4** (Me), 775 nm for **5** (OMe)]. The emission maximum of the alkylacetylide complex **6** (R = *t*-Bu, $\lambda_{max} = 786$ nm) is red-shifted from those of **1**−**5** (R = C_6H_4X-4). From the emission spectra of **3**, **7**, and **8** (Figure 6), it is noteworthy that the emission maximum slightly blue-shifts in energy with the increased conjugation and length of the acetylide ligand ($C{\equiv}CC_6H_4)_nC{\equiv}CPh$ [$\lambda_{max} = 758$ nm for **3** ($n = 0$), 749 nm for **7** ($n = 1$), 748 nm for **8** ($n = 2$)], and the difference in energy from **3** to **8** is 176 cm^{-1}.

Complexes **9** and **10** are nonemissive in CH_2Cl_2 solution at room temperature, but they are emissive in glassy *n*-butyronitrile solution at 77 K and the solid state (298 and 77 K). Excitation of **9** and **10** at $\lambda = 415$ nm in *n*-butyronitrile glass at 77 K produces red emission with $\lambda_{max} = 597$ and 615 nm, respectively. In the solid state, **9** and **10** emit at 616 and 630 nm at 77 K and 649 and 711 nm at 298 K, respectively. The glassy emission for **9** and **10** was studied in *n*-butyronitrile rather than MeOH/EtOH because the solubility of **9** and **10** in alcoholic solutions is poor. The glassy emission of **9** at 77 K was also investigated in CH_2Cl_2/toluene (1/1, v/v) solution, and the emission maximum is detected at 592 nm, which is similar to that measured in *n*-butyronitrile.

Discussion

General Remarks. Acetylide- and carbene-ruthenium(II) complexes containing the tpy-bpy ligand set have been prepared in this work. $[(tpy)(bpy)Ru(H_2O)]^{2+}$ was used as the precursor rather than $[(tpy)(bpy)RuCl]^+$ because the latter does not react with acetylene substrates in the presence of Et_3N. For the syntheses of the acetylide complexes, the choice of solvent is critical. It was found that the yield of the acetylide complexes was low (ca 10%) when the reaction was performed in MeOH or EtOH. When CH_3CN or CH_2Cl_2 was used, $[(tpy)(bpy)Ru(NCCH_3)]^{2+}$ or $[(tpy)(bpy)RuCl]^+$ was isolated as the major product, respectively. We found that acetone was the best solvent for this procedure, and yields of around 60−80% were generally obtained. This is presumably because acetone is a noncoordinating (or very poor) ligand for the $[(tpy)(bpy)Ru]^{2+}$ moiety compared to CH_3CN and Cl^-.

There are several accounts of vinylidene-ruthenium complexes that are unstable toward interaction with alcohol to give alkoxycarbene-ruthenium complexes.[28] For example, Bruce and co-workers reported that $[Cp(PPh_3)(PMe_3)Ru{=}C{=}CHPh]PF_6$ reacts with methanol to give $[Cp(PPh_3)(PMe_3)Ru{=}C(OMe)CH_2Ph]PF_6$.[29] In this work, we pursued the vinylidene derivatives $[(tpy)(bpy)Ru{=}C{=}CHR]^{2+}$ as precursors for alkoxycarbene species.

(27) Manna, J.; John, K. D.; Hopkins, M. D. *Adv. Organomet. Chem.* **1995**, *38*, 79.
(28) Bruce, M. I. *Chem. Rev.* **1991**, *91*, 197.
(29) Bruce, M. I.; Swincer, A. G. *Aust. J. Chem.* **1980**, *33*, 1471.

Preparation of vinylidene derivatives was attempted in CH_2Cl_2 by (1) reacting HC≡CR with $[(tpy)(bpy)Ru(OH_2)](ClO_4)_2$ in the absence of Et_3N and (2) treating $[(tpy)(bpy)RuC{\equiv}CR]ClO_4$ with HCl or CF_3COOH. However, no vinylidene product was isolated from these routes. We reasoned that the vinylidene derivatives may be too reactive to be isolated, and we therefore attempted to prepare the alkoxycarbene species by reacting CF_3COOH with $[(tpy)(bpy)RuC{\equiv}CR]ClO_4$ in the presence of MeOH; we envisioned that this may generate the vinylidene intermediate in situ, which would react with MeOH to give the methoxycarbene complex. Hence the isolated product was the targeted carbene complexes $[(tpy)(bpy)Ru{=}C(OMe)(CH_2R)]^{2+}$ (**9** and **10**).

Electrochemical Information and Comparisons with $[(tpy)(bpy)RuL]^{n+}$. The acetylide complexes **1**−**8** show two reversible/quasi-reversible reduction waves at $E_{1/2} = -2.22$ to -2.14 and -1.95 to -1.87 V, plus an irreversible oxidation wave at $E_{pa} = 0.15$ to 0.26 V (scan rate = 50 mV s^{-1}), whereas the carbene complexes **9** and **10** show three reversible/quasi-reversible couples at $E_{1/2} = -2.03$ and -2.04, -1.57 and -1.50, and 0.99 and 1.00 V, respectively. The reduction waves for complexes **1**−**10** are assigned as reduction of the polypyridyl ligands, while the oxidation waves are assigned as metal-centered Ru(III/II) oxidations. The more positive $E_{1/2}$ values of the redox couples for **9** and **10** compared to **1**−**8** can be rationalized by the increase in electronic charge in the complexes. In the literature, the electrochemical behavior of ruthenium-polypyridyl complexes with the general formula $[Ru(tpy)(bpy)L]^{n+}$ have been extensively studied.[12,30] Complexes of this type show reduction waves corresponding to successive reduction at the polypyridyl ligands. The tpy ligand is preferentially reduced because its π* level is lower than that of bpy. With reference to previous works, we assign the more negative reduction couples at $E_{1/2} = -2.22$ to -2.14, -2.03, and -2.04 V (for **1**−**8**, **9**, and **10**, respectively) to the reduction of the bpy ligand, and the other reduction couple at $E_{1/2} = -1.95$ to -1.87, -1.57, and -1.50 V (for **1**−**8**, **9**, and **10**, respectively) to tpy reduction.

The irreversible oxidation waves for **1**−**8** are assigned as metal-centered, because the coordinated tpy or bpy ligands in $[Ru(tpy)(bpy)L]^{n+}$ are not oxidized at around this potential. Comparing the reported Ru(III/II) redox potentials of $[Ru(tpy)(bpy)L]^+$ (L = $^-$Cl,[12c] $^-$NCNAr,[30b] and $^-$C≡N:[12e] $E_{1/2}$ = 0.41, 0.34−0.43, and 0.67 V, respectively) and E_{pa} of $[Ru(tpy)(bpy)C{\equiv}CR]^+$ (0.15 to 0.26 V), $[Ru(tpy)(bpy)C{\equiv}CR]^+$ is clearly more easily oxidized. It is interesting to compare the Ru(III/II) waves for $[Ru(tpy)(bpy)C{\equiv}CR]^+$ and $[Ru(tpy)(bpy)C{\equiv}N]^+$, because $^-$C≡CR and $^-$C≡N are isoelectronic and both ligands can coordinate with metal centers through σ-bonding and π-back-bonding interactions. We have observed that the oxidation of $[Ru(tpy)(bpy)C{\equiv}CR]^+$ occurs at more cathodic potentials than that of $[Ru(tpy)(bpy)C{\equiv}N]^+$, which reflects the nature of $^-$C≡CR as a stronger σ-donating and weaker π-accepting ligand than $^-$C≡N. This correlates with the spectroscopic data (see below), which shows that the Ru(II) → π*(polypyridyl) ^{1}MLCT absorption band for $[Ru(tpy)(bpy)C{\equiv}CR]^+$ (λ_{max} = 513−526 nm) is red-shifted from that for $[Ru(tpy)(bpy)C{\equiv}N]^+$ (λ_{max} = 470 nm).[12e]

The $E_{1/2}$ values of the Ru(III/II) oxidation couple for $[(tpy)(bpy)Ru{=}C(OMe)(CH_2R)]^{2+}$ (**9** and **10**) are 0.99 and 1.00 V, respectively, which are slightly higher than those for $[(tpy)(bpy)Ru(py)]^{2+}$ and $[(tpy)(bpy)Ru(NCCH_3)]^{2+}$ (0.86 and 0.89 V, respectively).[30a] The crystallographic data indicate that the methoxyalkylcarbene group in this work is a Fischer-type carbene, which can coordinate to metal centers through σ and π-back-bonding interactions like pyridine and CH_3CN. These data suggest that methoxyalkylcarbene ligands can stabilize the Ru(II) center more effectively than pyridine and CH_3CN. This is also consistent with the spectroscopic data (see below), which depicts the Ru(II) → π*(polypyridyl) ^{1}MLCT absorption for $[Ru(tpy)(bpy){=}C(OMe)(CH_2R)]^{2+}$ (λ_{max} = 415 (**9**) and 408 (**10**) nm) at a higher energy than that for $[Ru(tpy)(bpy)(py)]^{2+}$ and $[(tpy)(bpy)Ru(NCCH_3)]^{2+}$ (λ_{max} = 466 and 455 nm, respectively).[30a] The reversibility of the Ru(III)/(II) couple for **9** and **10** shows that the coordinated Fischer carbene ligand is stable, at least during the cyclic voltammetric scans, in the oxidizing Ru(III) complexes with an oxidation potential of 0.99 and 1.00 V, respectively.

Electronic and Emission Spectroscopy. In the literature, polypyridyl complexes of ruthenium(II) feature two types of absorption bands: highly intense absorptions in the UV region and moderately intense absorptions in the visible region. The former are attributed to intraligand (polypyridyl) π → π* transitions, while the latter are ascribed to $d_\pi(Ru^{II})$ → π*(polypyridyl) charge transfer (MLCT) transitions.[1d] In this work, the absorption bands in the visible region for **1**−**10** are assigned to $d_\pi(Ru^{II})$ → π*(polypyridyl) ^{1}MLCT transitions. However, we note that for the $[(tpy)(bpy)RuC{\equiv}CR]^+$ complexes, this MLCT transition slightly blue-shifts in energy (by 909 cm^{-1}) as the π-conjugation length of the arylacetylide ligand increases: λ_{max} for R = C_6H_4X-4 > $C_6H_4C{\equiv}CPh$ > $(C_6H_4C{\equiv}C)_2Ph$. This suggests that the HOMO may contain a contribution from the acetylide ligand. Indeed, the decrease in π* energy for more conjugated arylacetylide ligands would result in enhanced metal-to-ligand (Ru-to-acetylide) π-back-bonding and a decrease in electron density around Ru, leading to a larger energy gap between the Ru(II) d_π orbitals and polypyridyl π* orbitals. The alternative assignment for the visible absorptions to $d_\pi(Ru^{II})$ → π*(C≡CAr) transitions for **1**−**8** is unreasonable because the analogous transition for *trans*-$[Ru(16\text{-}TMC)(C{\equiv}CC_6H_4X\text{-}p)_2]$ (X = F, Cl, H, Me, and OMe) occurs at λ_{max} = 379−408 nm.[22a] In any case, the Ru → π*(C≡CAr) MLCT transition for polypyridine complexes should appear at a higher energy than for derivatives supported by 16-TMC because 16-TMC is a stronger σ-donor and weaker π-acceptor than polypyridines.

The Ru(II) → π*(polypyridyl) ^{1}MLCT transitions for **1**−**8** are noticeably different from those of **9** and **10** (415 and 408 nm, respectively). Indeed the MLCT transition for $[(tpy)(bpy)RuL]^{n+}$ is sensitive to the nature of the ligand L. For example, the Ru(II) → π*(polypyridyl) transitions for $[Ru(tpy)(bpy)(N{\equiv}CCH_3)]^{2+}$,[30a] $[Ru(tpy)(bpy)(py)]^{2+}$,[30a] $[Ru(tpy)(bpy)(C{\equiv}N)]^+$,[12e] $[Ru(tpy)(bpy)$-

(30) (a) Rasmussen, S. C.; Ronco, S. E.; Mlsna, D. A.; Billadeau, M. A.; Pennington, W. T.; Kolis, J. W.; Petersen, J. D. *Inorg. Chem.* **1995**, *34*, 821. (b) Mosher, P. J.; Yap, G. P. A.; Crutchley, R. J. *Inorg. Chem.* **2001**, *40*, 550.

$(NCNAr)]^+$,[30b] and $[Ru(tpy)(bpy)Cl]^+$ [12c] occur at λ_{max} = 455, 466, 470, 489−496, and 502 nm, respectively. The λ_{max} of the ^{1}MLCT transitions for **1**−**8** (502−526 nm) are clearly red-shifted in energy in comparison; this is consistent with the greater σ-donating ability of the $^-$C≡CR ligand, which destabilizes the d_π(Ru) energy levels. The blue-shifted absorption maximum of the ^{1}MLCT transitions for **9** and **10** reflects the greater π-accepting ability of the [:C(OMe)(CH_2R)] Fischer carbene moieties. The Ru → π*(carbene) π-back-bonding interaction would stabilize the d_π(Ru) orbitals, leading to an increase in energy for the d_π → π*(polypyridine) charge transfer transition. However, the extent of the π-back-bonding interaction is not as substantial as that in $[Ru(tpy)(bpy)(CO)]^{2+}$ (λ_{max} = 368 nm).[12c]

In the literature, ruthenium(II) complexes of terpyridine ligand(s) are typically nonemissive or weakly emissive with short excited-state lifetimes at room temperature. This has been attributed to effective radiationless decay from low lying ^{3}MC (metal-centered) excited states.[1d] In this work, excitation of **1**−**8** at λ = 550 nm in CH_3CN at 298 K gave emission at λ_{max} = 748−786 nm, and the energy of the emission maximum increases in the order R = *t*-Bu (12 720 cm^{-1}) < C_6H_4X-4 (12 900−13 330 cm^{-1}) ≤ $C_6H_4C{\equiv}CPh$ (13 350 cm^{-1}) ≈ $(C_6H_4C{\equiv}C)_2Ph$ (13 370 cm^{-1}). Moreover, the emission maximum for R = C_6H_4X-4 partially blue-shifts in energy (by 430 cm^{-1}) as the electron-donating ability of X decreases in the order: λ_{max} for X = OMe < Me < H < F ≈ Cl. The anomalous effect of the fluoro substituent can be rationalized by its negative inductive and positive mesomeric effects. Excitation of **9** and **10** at λ = 415 nm in *n*-butyronitrile at 77 K produces emission at λ_{max} = 597 and 615 nm, respectively. As the trend in emission maxima for **1**−**8** parallels the corresponding Ru(II) → π*(polypyridyl) ^{1}MLCT absorption maxima, and the red-shift in emission maxima from the carbene complexes **9** and **10** to the acetylide complexes **1**−**8** is also reflected in the red-shift in Ru(II) → π*(polypyridyl) ^{1}MLCT transition from **9** and **10** to **1**−**8**, these emissions are tentatively ascribed as $d_\pi(Ru^{II})$ → π*(polypyridyl) ^{3}MLCT in nature.

Summary

A series of acetylide- and methoxyalkylcarbene-ruthenium(II) complexes supported by the tpy-bpy ligand set have been synthesized. The molecular structures of **4**(PF_6), **5**(PF_6), and **9**(ClO_4)$_2$ have been characterized by X-ray crystallography. The absorption bands in the visible region for **1**−**8** (λ_{max} = 502−526 nm) and **9** and **10** (λ_{max} ca. 410 nm) are assigned as $d_\pi(Ru^{II})$ → π*(polypyridyl) ^{1}MLCT transitions, while the emissions of complexes **1**−**8** at λ_{max} = 748−786 nm in CH_3CN solution at 298 K (λ_{ex} = 550 nm) are tentatively assigned as $d_\pi(Ru^{II})$ → π*(polypyridyl) ^{3}MLCT in nature. Comparisons of their electrochemical and spectroscopic data with those of related $[(tpy)(bpy)RuL]^{n+}$ derivatives suggest that acetylide ligands are strong σ-donors while methoxyalkylcarbene ligands are better π-acceptors than pyridine and CH_3CN. The Fischer-type carbene complexes **9** and **10** undergo photochemical reaction upon irradiation in CH_3CN and CH_2Cl_2, and $[(tpy)(bpy)RuN{\equiv}CCH_3]^{2+}$ and 4-methoxybenzaldehyde were characterized as reaction products from the photolysis of **9** in CH_3CN.

Acknowledgment. This work was supported by the Research Grants Council of the Hong Kong SAR, China (HKU 7077/01P), the Croucher Foundation (Hong Kong), and The University of Hong Kong.

Supporting Information Available: Characterization data; crystal data for **4**(PF_6)·2½CH_3CN, **5**(PF_6), and **9**(ClO_4)$_2$·2CH_2Cl_2; perspective view of cation in **5**; absorption and emission spectra of **3** in CH_2Cl_2; UV−visible spectral trace for photolysis of **9** in CH_2Cl_2. This material is available free of charge via the Internet at http://pubs.acs.org.

OM034379K